CFD modelling of different properties of nanofluids in header and riser tube of flat plate solar collector

CFD modelling of different properties of nanofluids in header and riser tube of flat plate solar collector

K Farhana [1,3*], K Kadirgama[1], M M Noor[1], M M Rahman[1], D Ramasamy[1],and A S F Mahamude[2]

[1]Faculty of Mechanical Engineering, Universiti Malaysia Pahang, 26600 Pekan, Pahang, Malaysia
[2]Faculty of Chemical & Natural Resources Engineering, Universiti Malaysia Pahang, 26300 Gambang, Pahang, Malaysia
[3]Department of Apparel Manufacturing Engineering, Bangladesh University of Textiles, Dhaka 1208, Bangladesh

[*]Corresponding author: kanizfar7@gmail.com

Abstract. This paper aimed to evaluate the state of three different flow parameters of nanofluids and hybrid nanofluids flowing through inside header and riser tube of flat plate solar collector. This research work studied with Computational fluid dynamics (CFD) modelling method using nanofluids (Al_2O_3, TiO_2, ZnO) and hybrid nanofluids (Al_2O_3+TiO_2, TiO_2+ZnO, ZnO + Al_2O_3). The modelling was three dimensional under k-epsilon turbulence model, which was set with Standard and Standard Wall Functions. Besides, Absolute reference frame and calculative intensity percentage was fixed. The base fluid was water as well as volume fraction of nanofluids and hybrid nanofluids was 0.1%. Single-phase viscous model with energy equation used. Three types of design models (Model A, B and C) used with fixed inlet and outlet diameter. The number of header tubes fixed with two, but the number of riser tube varied such as two, seven and twelve. Maximum dynamic pressure increased in model B for both nanofluid and hybrid nanofluid of about 48% and 16% respectively. Velocity magnitude enhanced in maximal for both nanofluid and hybrid nanofluid in model B. Besides, highest turbulence kinetic energy achieved in model A (5.5%) for nanofluids and in model B (18%) for hybrid nanofluids. Model B perform better comparing with model A and model C.

1. Introduction

Depletion of fossil fuel and its negative impact on to the environment is the burning issue of today's earth. As consequences renewable energies are now taking the place of fossil energies. Among all renewable energies solar energy is the most promising due to its availability [1]. The Green technology made a revolution to overcome these severe problems. Academic and industrial personnel are working hard to establish the basement of renewable energies all around. As a result computational numerical simulation revealed as an important tool for the improvement of industrial production chain and production process optimization [2, 3]. In case of solar energy various computational simulations done for the replacement of fossil energy strongly [4-6]. In solar energy system, solar collector devices absorb the solar flux which incident on the surface and transfer the energy as heat into the working fluid flowing through them [7]. Flat plate solar collector is relatively simple and widest in application to heat the water

[8]. Generally flat plate solar collector made of glass, absorber, riser and header pipes, insulator, back sheet, aluminium rails. Ultrasonically welded absorber with riser pipes used to transfer the heat to the working fluid. The riser pipe and the header pipe are fixed together with to form a harp-shaped heat exchanger inside which the working fluid can flow [9, 10]. Applying nano sized particles in working fluids along with others can improve the performance of flat plate solar collector [11, 12].

Nanometer sized materials dispersed in base fluid such as water and oil produced nanofluids [13, 14]. Moreover, hybrid nanofluid is the new extended field of nanoscience. Basically this new composite is prepared with two or more substances having different physical and chemical properties mixed in a homogenous phase [15, 16]. Nanofluids dramatically change the heat transfer rate and thermal conductivity properties of any substance. These characteristics mostly depend on size, shape, density, surface energy, and thermophysical properties of nano particles. In addition, nanofluids exhibit good stability, improved surface volume and less sedimentation of particles. As well as increased volume concentration of nanoparticles and temperature can increase the thermal conductivity. Besides different nanoparticles show individual performance of thermal conductivity such as metallic nanoparticles perform higher thermal conductivity than non-metallic nano particles. Recently some literatures revealed hybrid nanofluids remarkably can change the thermal conductivity and which is superior to single phase nanofluids [17, 18]. In addition, before going to practical operations; computer-based numerical simulation can be done repeatedly by creating virtual design model to reduce the cost of any project. Numerical simulation can be done by Computational Fluid Dynamics (CFD) systems of different objects such as fluid flow, heat transfer and chemical reactions as well [19, 20]. Similarly, a considerable number of literatures published on flat plate solar collectors from computational simulation standpoint [21, 22].

In this research study, dynamic pressure, velocity magnitude and turbulence kinetic energy of nanofluids (Al_2O_3, TiO_2, and ZnO) and hybrid nanofluids (Al_2O_3 + TiO_2, TiO_2+ZnO and ZnO + Al_2O_3) flowing through the pipes with constant temperature boundary condition investigated. Recently some researchers used nanofluids as working fluid in replace of water. So, there is a possibility to use hybrid nanofluids as working fluid also. Prior to practical application, computational simulation is beneficial to observe the fluid properties of hybrid nanofluids along with nanofluids and it will also reduce the cost to do the repeated practical implementation. Moreover, various designs (header and riser tube) are available in literature; to obtain optimum design for nanofluids and hybrid nanofluids numerical simulation is very persuasive. For computer-based simulations three types of design models were prepared using “SOLIDWORKS” software. The ANSYS R15.0 software used to perform numerical simulations. The turbulence k-epsilon model was set, and the results reviewed in Post Processing step of ANSYS Fluent.

2. Physical properties of nanofluids and hybrid nanofluids

According to mixing theory, density of nanofluids measured by [24],

$$\rho_{nf} = \varphi \rho_p + (1-\varphi)\rho_f \tag{1}$$

And density of hybrid nanofluids [25]

$$\rho_{hnf} = \phi_{nf1}\rho_{nf1} + \phi_{nf2}\rho_{nf2} + (1-\phi)\rho_{bf} \tag{2}$$

Based on thermal equilibrium, specific heat of nanofluids [26] and hybrid nanofluids [27] as,

$$c_{p,nf} = \frac{\varphi(\rho c_p)_p + (1-\varphi)(\rho c_p)_f}{\rho_{nf}} \tag{3}$$

$$C_{hnf} = \frac{\varphi_{nf1}\rho_{nf1}c_{nf1} + \varphi_{nf2}\rho_{nf2}c_{nf2} + (1-\varphi)\rho_{bf}c_{bf}}{\rho_{hnf}} \tag{4}$$

Thermal conductivity of nanofluids [28] and hybrid nanofluids [25] can be calculated by the following equations in successive,

$$\frac{k_{nf}}{k_{nf}} = \frac{k_p + 2k + 2\varphi(k_p - k_{bf})}{k_p + 2k - \varphi(k_p - k)} \tag{5}$$

$$K_{hnf} = K_{bf}\left[\frac{\frac{(\phi_{np1}k_{np1} + \phi_{np2}k_{np2})}{\phi_{hnf}} + 2k_{bf} + 2(\phi_{np1}k_{np1} + \phi_{np2}k_{np2}) - 2\phi k_{bf}}{\frac{(\phi_{np1}k_{np1} + \phi_{np2}k_{np2})}{\phi_{hnf}} + 2k_{bf} - 2(\phi_{np1}k_{np1} + \phi_{np2}k_{np2}) + \phi k_{bf}}\right] \tag{6}$$

According to Einstein model, viscosity of suspension increases linearly with the augmentation of nanoparticles in the suspension [29],

$$\mu_{nf} = (1 + 2.5\varphi)\mu_{bf} \tag{7}$$

Theoretical values of density, specific heat, thermal conductivity and viscosity obtained using the above equations from one to seven for water, nanofluids and hybrid nanofluids and illustrated in Table 1.

Table 1. Physical properties of water, nanofluids and hybrid nanofluids.

Properties	**Water**	**Al_2O_3**	**TiO_2**	**ZnO**	**Al_2O_3 + TiO_2**	**TiO_2 + ZnO**	**ZnO Al_2O_3 +**
Density (kg/m^3)	998.2	1294.38	1321.38	1458.38	1029.17	1037.37	1036.018
Specific heat (j/kg.k)	4182	3139.057	3064.781	2769.194	4044.685	4011.528	4017.409
Thermal conductivity (W/m.k)	0.6	0.79	0.76	0.79	0.64	0.64	0.64
Viscosity (kg/m.s)	0.001003	0.001253	0.001253	0.001253	0.001315	0.001315	0.001315

3. CFD theory and equations

In this study the flow pattern with constant temperature through a combined structure of two circular tubes simulated using FLUENT software ANSYS R15.0. Here only single-phase model used for simulations. Simulations carried out in steady state conditions solving mass, momentum and energy conservation equations as well as viscous model of transportation [30]:

Continuity Equation

$$\frac{\partial \rho}{\partial t} + \nabla \cdot (\rho U) = 0 \tag{8}$$

Momentum equation:

$$\frac{\partial}{\partial t}(\rho U)+\nabla\cdot(\rho UU)=-\nabla P+\nabla\tau+\rho g \tag{9}$$

Energy Equation:

$$\frac{\partial}{\partial t}(\rho h)+\nabla\cdot(\rho U c_p T)=\nabla\cdot(k\nabla T) \tag{10}$$

Viscous Model:
K-epsilon model is the most common for turbulent flows which is very easy to converge and implement as well. Turbulence kinetic energy, k and turbulent dissipation rate, ε are obtained from the following transport equations,

$$\frac{\partial}{\partial t}(\rho k)+\frac{\partial}{\partial x_i}(\rho k u_i)=\frac{\partial}{\partial x_i}\left[\left(\mu+\frac{\mu_t}{\sigma_k}\right)\frac{\partial k}{\partial x_j}\right]+P_k+P_b-\rho\varepsilon-Y_M+S_k \tag{11}$$

$$\frac{\partial}{\partial t}(\rho\varepsilon)+\frac{\partial}{\partial x_i}(\rho\varepsilon u_i)=\frac{\partial}{\partial x_i}\left[\left(\mu+\frac{\mu_t}{\sigma_\varepsilon}\right)\frac{\partial\varepsilon}{\partial x_j}\right]+C_{1\varepsilon}\frac{\varepsilon}{k}(P_k+C_{3\varepsilon}P_b)-\rho C_{2\varepsilon}\frac{\varepsilon^2}{k}+S_\varepsilon \tag{12}$$

4. Modelling

4.1 Design Modeler
In design modeler, the geometries were imported rather than directly created here. The diameters of header and riser tube of flat plate solar collector were fixed in this study. But the number of riser tube was two, seven and twelve whereas the number of header tube fixed with two. The three-dimensional geometry of header and riser tube is created by SOLIDWORKS software (version 2016) and Table 2 presents the parameters accordingly. Figure 1 shows the combined sketch of header and riser tube of flat plate solar collector which is model A, model B and model C respectively.

Table 2. Parameters of header and riser tubes of flat plate solar collector.

Parameters	**Dimension**	
	Header Tube	**Riser Tube**
Diameter (mm)	22	10
Thickness (mm)	0.6	0.45
Length (mm)	900	1714
Number of tubes	2	2, 7 and 12

4.2 Meshing
Meshing is the most critical and meshing elements and grid of cells are subjected to solve the fluid flow equations [31]. Here Tetrahedrons meshing in header tube and CutCell meshing in riser is done automatically in the three-dimensional computational domain. Figure 2 represents the meshed 3D model of header and riser tube.

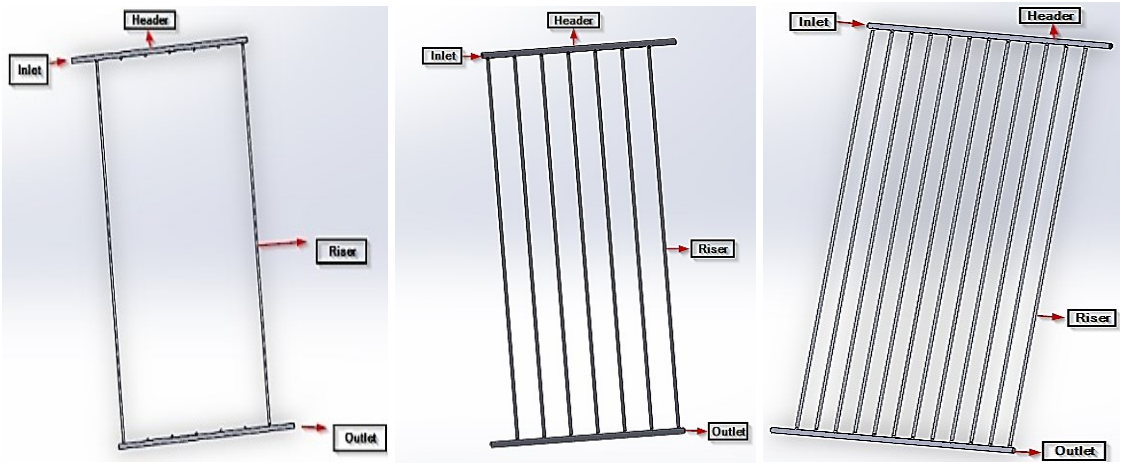

(a) Model A (b) Model B (c) Model C

Figure 1. Schematic 3-D view of consolidated header and riser tubes

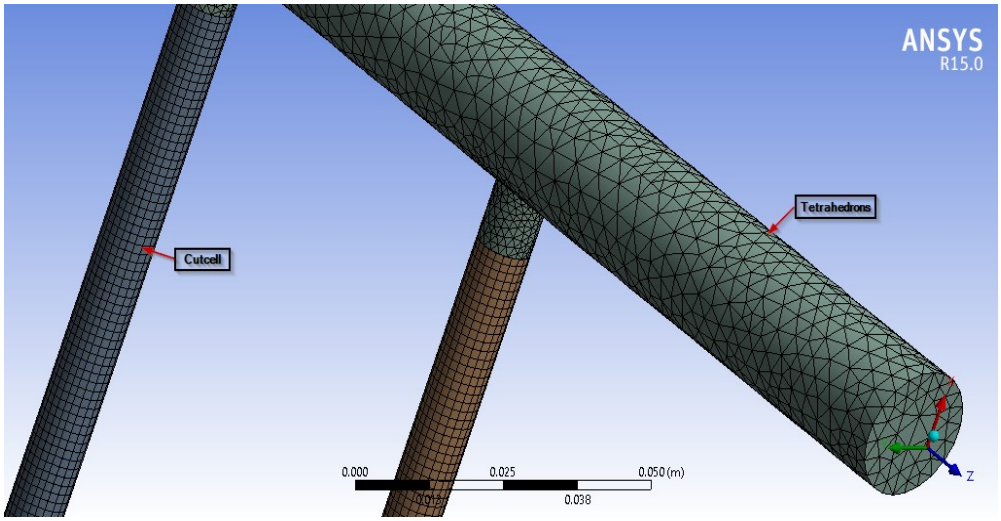

Figure 2. 3D meshing model.

4.3 Solution Setup and Solution Calculation

In this present work, Pressure-based, Absolute-velocity and Steady solver used for solution calculation. Setting of models is very important for computational simulations [32]. Here Energy Equation, Viscous-Standard k-epsilon and Standard Wall Functions used. Before setting the models Reynolds number and flow behaviour done theoretically by the following equation [33];

$$\mathrm{Re} = \frac{\rho D v}{\mu} \tag{13}$$

In Boundary Conditions, velocity-inlet and pressure-outlet was set. For all types of fluids, velocity fixed with 0.25 m/s and hydraulic diameter was 0.022 m. Turbulent Intensity% calculated by (Eq(14)) [34].

$$\text{Turbulent Intensity} = 0.16 \times (\mathrm{Re})^{\left[-\frac{1}{8}\right]} \times 100\% \tag{14}$$

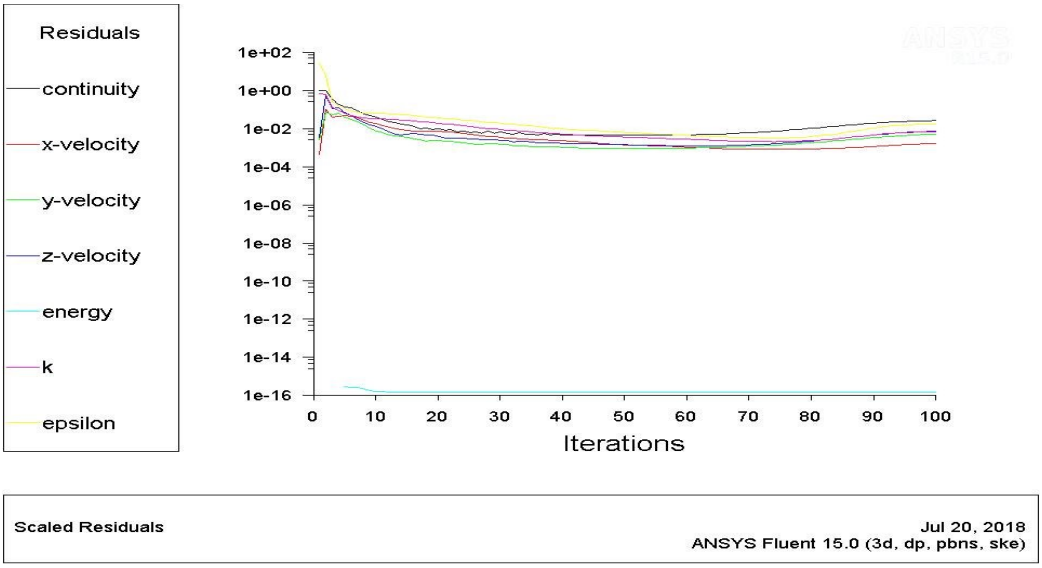

Figure 3. Converge Solution.

Solution calculation was performed based on pressure-velocity coupling with Simple Scheme and Spatial Discretization. Figure 3 illustrates the converged solution of the simulation.

5. Result and Discussion

In this study, the result of the simulation has been presented in both graphical views (contour plot) and data interpretations. In CFD post processing blue colour define the lowest value and red is the highest value [35]. Figure 4 shows the contours of the three geometries in pressure variable.

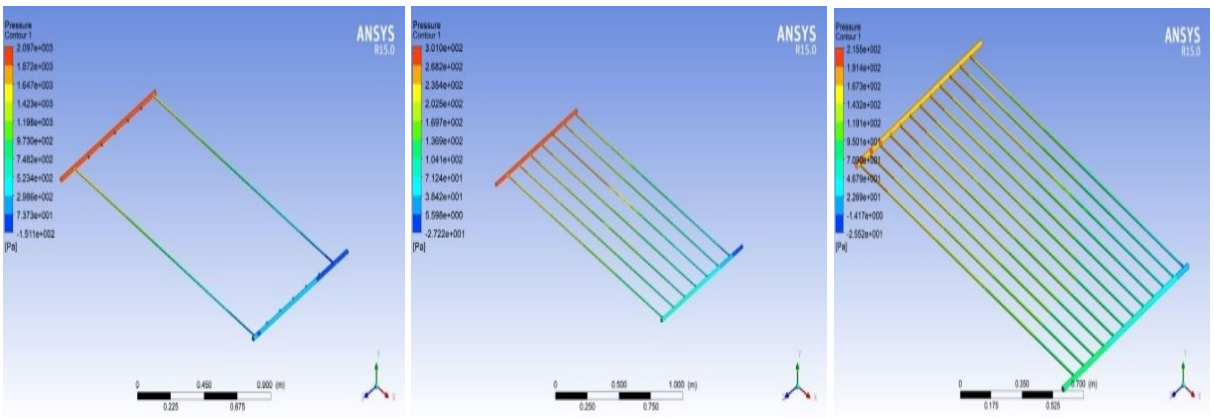

(a) Model A (b) Model B (c) Model C

Figure 4. Results of pressure (contours)

Three types of resulting data such as dynamic pressure, velocity magnitude and turbulence kinetic energy were accumulated in maximum type by CFD reports with volume integrals in case of water, nanofluids and hybrid nanofluids. The numerical values of these properties have been showed in Table 3 according to model A, model B and model C.

Table 3. Computational values of different properties of model A, model B and model C.

Characteristics	Dynamic Pressure (Pascal			Velocity Magnitude (m/s)			Turbulence Kinetic Energy (m2/s2)		
	Model A	Model B	Model C	Model A	Model B	Model C	Model A	Model B	Model C
Water	438.07	86.74	71.03	0.9368	0.4168	0.3772	0.0895	0.0122	0.0105
Nanofluids									
Al_2O_3	561.64	115.16	81.83	0.9315	0.4218	0.3555	0.0945	0.0123	0.0099
TiO_2	592.36	117.64	83.17	0.9468	0.4219	0.3548	0.0921	0.0125	0.0098
ZnO	636.99	129.09	94.47	0.9346	0.4207	0.3580	0.0940	0.0123	0.0100
Hybrid nanofluids									
Al_2O_3+TiO_2	439.84	90.79	60.82	0.9245	0.4200	0.3438	0.0960	0.0144	0.0092
TiO_2+ZnO	447.46	100.88	61.19	0.9288	0.4410	0.3434	0.0950	0.0126	0.0092
ZnO + Al_2O_3	444.58	90.272	61.33	0.9264	0.4174	0.3441	0.0941	0.0128	0.0093

Here volume fraction 0.1% of nanofluids and hybrid nanofluids was studied. Model k-epsilon turbulence utilized for numerical analysis as this model can avoid the coarse data in a convenient way. Although all the models have same inlet and outlet flow diameter (22mm), however the quantity of riser tubes varied, and simulation was performed in fully developed condition. Flow parameters such as dynamic pressure, velocity magnitude and turbulence kinetic energy studied.

Table 3 illustrates that model A, model B and model C shows maximum increment of dynamic pressure for ZnO nanofluids of about 45%, 48% and 33% respectively. In case of hybrid nanofluids, model A and model B performs the highest improvement of dynamic pressure with TiO_2+ZnO around 2.1% and 16% accordingly. Whereas model C shows decrement of dynamic pressure of 14% in maximum with Al_2O_3+TiO_2 hybrid nanofluid. Besides, velocity magnitude increases in maximal around 1.0% and 1.2% with TiO_2 nanofluid in model A and model B respectively. But it is decreased in model C of about 5.9% with TiO_2 nanofluid. TiO_2+ZnO hybrid nanofluid performs the best increment (5.8%) of velocity magnitude in model B but declined in maximum (8.9%) in model C. Similarly, model A shows velocity magnitude declination (1.3%) with Al_2O_3+TiO_2 hybrid nanofluid. And finally, turbulence kinetic energy increased in model A and model B for both nanofluid and hybrid nanofluids. Model A presents the raise of turbulence kinetic energy of about 5.5% and 7.2% with Al_2O_3 nanofluid and Al_2O_3+TiO_2 hybrid nanofluid respectively, while model B exhibited 2.4% and 18% enhancement with TiO_2 nanofluid and Al_2O_3+TiO_2 hybrid nanofluid. On the other hand, model C shows negative performance for both nanofluids (TiO_2) and hybrid nanofluids (All) of about 6.6% and 12% respectively in highest condition.

In addition, Figure 5, Figure 6 and Figure 7 illustrate the contours of dynamic pressure, velocity magnitude and turbulence kinetic energy for nanofluids and hybrid nanofluids in inlet and outlet of Model A and these schematic views are more or less similar for all models.

According to Mazumder [36], colour of contours present the development of solution. Red colour shows the fully developed solution whereas gradually blue colour represents the lowest value. Maïga, Nguyen, Galanis and Roy [37] numerically investigated in turbulent flow regime; heat transfer enhanced due to nanoparticles.

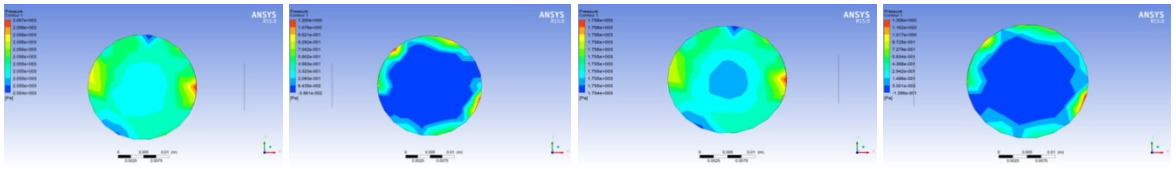

(a) (b) (c) (d)

Figure 5. Contours of Dynamic Pressure of Model A (a) inlet of nanofluid (b) outlet of nanofluid (c) inlet of hybrid nanofluid (d) outlet of hybrid nanofluid.

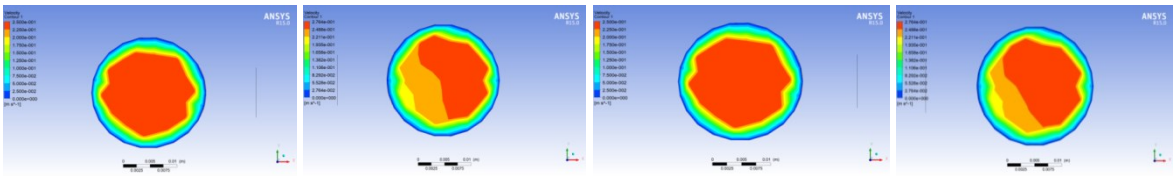

(a) (b) (c) (d)

Figure 6. Contours of Velocity Magnitude of Model A (a) inlet of nanofluid (b) outlet of nanofluid (c) inlet of hybrid nanofluid (d) outlet of hybrid nanofluid.

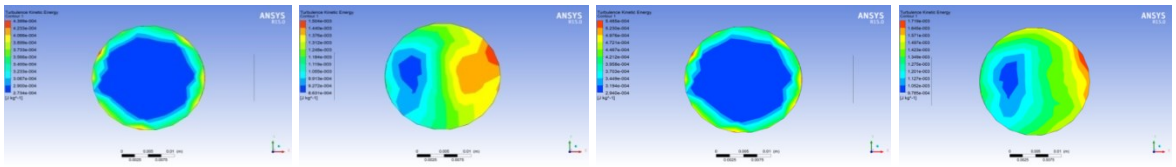

(a) (b) (c) (d)

Figure 7. Contours of Turbulence Kinetic Energy of Model A (a) inlet of nanofluid (b) outlet of nanofluid (c) inlet of hybrid nanofluid (d) outlet of hybrid nanofluid.

6. Conclusion

Three kinds of flow parameters of nanofluids and hybrid nanofluids flowing through inside of combined pipes (header and riser) investigated numerically using ANSYS R15.0. The numerical research revealed that dynamic pressure increased for nanofluids in all models but decreased in model C for hybrid nanofluids. Maximum 48% dynamic pressure increased for nanofluids and 16% increased for hybrid nanofluids in model B. Besides model B performs better in case of velocity magnitude for both nanofluid and hybrid nanofluid around 1.2% and 5.8% increment respectively. And finally, the most significant turbulence kinetic energy property shows good completion in model A and model B with both nanofluids and hybrid nanofluids. However, model A shows much better performance in turbulence kinetic energy enhancement around 5.5% for nanofluids and model B shows 18% improvement of it with hybrid nanofluids. Whereas it is dissimilar in model C and presents negative results for both nanofluid and hybrid nanofluids. From the above computational analysis of these three parameters of fluid flow, model B performs better than the others two models.

Acknowledgment

The authors would like to acknowledge University Malaysia Pahang (UMP), Ministry of Higher Education (MOHE) of Malaysia for Grants RDU 180328, RDU160152 and Bangabandhu Science and Technology Fellowship Trust (Bangladesh) for financial assistance, which made this study possible.

References

[1] Vasu A, Hagos F Y, Noor M, Mamat R, Azmi W, Abdullah A A and Ibrahim T K 2017 Corrosion effect of phase change materials in solar thermal energy storage application *Renewable and Sustainable Energy Reviews* **76** 19-33
[2] Canale M, Fagiano L and Milanese M 2009 KiteGen: A revolution in wind energy generation *Energy* **34** 355-61
[3] Khelifi S, Verschraegen J, Burgelman M and Belghachi A 2008 Numerical simulation of the impurity photovoltaic effect in silicon solar cells *Renewable Energy* **33** 293-8
[4] Villar N M, López J C, Muñoz F D, García E R and Andrés A C 2009 Numerical 3-D heat flux simulations on flat plate solar collectors *Solar energy* **83** 1086-92
[5] Hassan M M and Beliveau Y 2008 Modeling of an integrated solar system *Building and Environment* **43** 804-10
[6] Tingzhen M, Wei L, Guoling X, Yanbin X, Xuhu G and Yuan P 2008 Numerical simulation of the solar chimney power plant systems coupled with turbine *Renewable Energy* **33** 897-905
[7] Chang H, Duan C, Wen K, Liu Y, Xiang C, Wan Z, He S, Jing C and Shu S 2015 Modeling study on the thermal performance of a modified cavity receiver with glass window and secondary reflector *Energy Conversion and Management* **106** 1362-9
[8] Klevinskis A and Bucinskas V 2011 Analysis of a Flat-Plate Solar Collector *Mokslas: Lietuvos Ateitis* **3** 39
[9] Jamil M, Sidik N C and Yazid M M 2016 Thermal performance of thermosyphon evacuated tube solar collector using TiO2/water nanofluid *J. Adv. Res. Fluid Mech. Therm. Sci.* **20** 12-29
[10] Rommel M and Moock W 1997 Collector efficiency factor F'for absorbers with rectangular fluid ducts contacting the entire surface *Solar energy* **60** 199-207
[11] Sivakumar P, Raj W C, Malathi N J and Balakrishnan S 2013 Performance Analysis of Flat Plate Solar Water Heater by Changing the Heat Pipe Material. In: *Advanced Materials Research*: Trans Tech Publ) pp 64-9
[12] Verma S K, Tiwari A K and Chauhan D S 2016 Performance augmentation in flat plate solar collector using MgO/water nanofluid *Energy Conversion and Management* **124** 607-17
[13] Bhosale G and Borse S 2013 Pool Boiling CHF Enhancement with Al2 o 3-Cuo/H2 o Hybrid Nan fluid. In: *International Journal of Engineering Research and Technology*: IJERT)
[14] Sharif M Z, Azmi W H, Mamat R and Shaiful A I M 2018 Mechanism for improvement in refrigeration system performance by using nanorefrigerants and nanolubricants – A review *International Communications in Heat and Mass Transfer* **92** 56-63
[15] Yarmand H, Gharehkhani S, Ahmadi G, Shirazi S F S, Baradaran S, Montazer E, Zubir M N M, Alehashem M S, Kazi S and Dahari M 2015 Graphene nanoplatelets–silver hybrid nanofluids for enhanced heat transfer *Energy Conversion and Management* **100** 419-28
[16] Zawawi N N M, Azmi W H, Redhwan A A M, Sharif M Z and Samykano M 2018 Experimental investigation on thermo-physical properties of metal oxide composite nanolubricants *International Journal of Refrigeration* **89** 11-21
[17] Noghrehabadi A, Hajidavaloo E and Moravej M 2016 Experimental investigation of efficiency of square flat-plate solar collector using SiO 2/water nanofluid *Case Studies in Thermal Engineering* **8** 378-86
[18] Kasaeian A, Eshghi A T and Sameti M 2015 A review on the applications of nanofluids in solar energy systems *Renewable and Sustainable Energy Reviews* **43** 584-98
[19] Versteeg H K and Malalasekera W 2007 *An introduction to computational fluid dynamics: the finite volume method*: Pearson Education)
[20] Baukal Jr C E, Gershtein V and Li X J 2000 *Computational fluid dynamics in industrial combustion*: CRC press)

[21] Martinopoulos G, Missirlis D, Tsilingiridis G, Yakinthos K and Kyriakis N 2010 CFD modeling of a polymer solar collector *Renewable Energy* **35** 1499-508
[22] Sultana T, Morrison G L and Rosengarten G 2012 Thermal performance of a novel rooftop solar micro-concentrating collector *Solar Energy* **86** 1992-2000
[23] Gunjo D G, Mahanta P and Robi P 2017 CFD and experimental investigation of flat plate solar water heating system under steady state condition *Renewable Energy* **106** 24-36
[24] Drew D A and Passman S L 2006 *Theory of multicomponent fluids* vol 135: Springer Science & Business Media)
[25] Takabi B and Salehi S 2014 Augmentation of the heat transfer performance of a sinusoidal corrugated enclosure by employing hybrid nanofluid *Advances in Mechanical Engineering* **6** 147059
[26] Choi S U and Eastman J A 1995 Enhancing thermal conductivity of fluids with nanoparticles. Argonne National Lab., IL (United States))
[27] Abbasi S and Abbasi N 2000 The likely adverse environmental impacts of renewable energy sources *Applied Energy* **65** 121-44
[28] Suresh S, Venkitaraj K, Selvakumar P and Chandrasekar M 2011 Synthesis of Al 2 O 3–Cu/water hybrid nanofluids using two step method and its thermo physical properties *Colloids and Surfaces A: Physicochemical and Engineering Aspects* **388** 41-8
[29] Suresh S, Chandrasekar M and Sekhar S C 2011 Experimental studies on heat transfer and friction factor characteristics of CuO/water nanofluid under turbulent flow in a helically dimpled tube *Experimental Thermal and Fluid Science* **35** 542-9
[30] Versteeg H and Malalasekra W 1995 An introduction to computational fluid dynamics: the finite volume method approach *Harlow, England: Longman Scientific and Technical*
[31] Madenci E and Guven I 2015 *The finite element method and applications in engineering using ANSYS®*: Springer)
[32] Li B, He Z and Chen X 2008 Design, simulation and optimization of ANSYS Workbench *Press of Tsinghua University* 96-103
[33] Reynolds O 1883 XXIX. An experimental investigation of the circumstances which determine whether the motion of water shall he direct or sinuous, and of the law of resistance in parallel channels *Philosophical Transactions of the Royal Society of London* **174** 935-82
[34] Wilcox D C 1993 *Turbulence modeling for CFD* vol 2: DCW industries La Canada, CA)
[35] Sorokes J M, Hardin J and Hutchinson B 2016 A CFD Primer: What Do All Those Colors Really Mean? In: *Proceedings of the 45th Turbomachinery Symposium*: Turbomachinery Laboratories, Texas A&M Engineering Experiment Station)
[36] Mazumder Q H 2012 CFD analysis of single and multiphase flow characteristics in elbow *Engineering* **4** 210
[37] Maïga S E B, Nguyen C T, Galanis N and Roy G 2004 Heat transfer behaviours of nanofluids in a uniformly heated tube *Superlattices and Microstructures* **35** 543-57